Rapid Healing of Femoral Defects in Rats with Low Dose Sustained BMP2 Expression from PEGDA Hydrogel Microspheres

Corinne Sonnet,[1] C. LaShan Simpson,[2] Ronke M. Olabisi,[2] Kayleigh Sullivan,[1] ZaWaunyka Lazard,[1] Zbigniew Gugala,[3] John F. Peroni,[4] J. Michael Weh,[4] Alan R. Davis,[1,5,6] Jennifer L. West,[2] Elizabeth A. Olmsted-Davis[1,5,6]

[1]Center for Cell and Gene Therapy, Baylor College of Medicine, One Baylor Plaza, Alkek Building, Room N1010, Houston, Texas, 77030, [2]Department of Bioengineering, Rice University, Houston, Texas, 77030, [3]Department of Orthopedic Surgery and Rehabilitation, University of Texas Medical Branch, Galveston, Texas, 77555, [4]College of Veterinary Medicine, University of Georgia, Athens, Georiga, 30602, [5]Department of Pediatrics, Baylor College of Medicine, Houston, Texas, 77030, [6]Department of Orthopedic Surgery, Baylor College of Medicine, Houston, Texas, 77030

Received 7 January 2013; accepted 13 May 2013
Published online in Wiley Online Library (wileyonlinelibrary.com). DOI 10.1002/jor.22407

ABSTRACT: Current strategies for bone regeneration after traumatic injury often fail to provide adequate healing and integration. Here, we combined the poly (ethylene glycol) diacrylate (PEGDA) hydrogel with allogeneic "carrier" cells transduced with an adenovirus expressing BMP2. The system is unique in that the biomaterial encapsulates the cells, shielding them and thus suppressing destructive inflammatory processes. Using this system, complete healing of a 5 mm-long femur defect in a rat model occurs in under 3 weeks, through secretion of 100-fold lower levels of protein as compared to doses of recombinant BMP2 protein used in studies which lead to healing in 2–3 months. New bone formation was evaluated radiographically, histologically, and biomechanically at 2, 3, 6, 9, and 12 weeks after surgery. Rapid bone formation bridged the defect area and reliably integrated into the adjacent skeletal bone as early as 2 weeks. At 3 weeks, biomechanical analysis showed the new bone to possess 79% of torsional strength of the intact contralateral femur. Histological evaluation showed normal bone healing, with no infiltration of inflammatory cells with the bone being stable approximately 1 year later. We propose that these osteoinductive microspheres offer a more efficacious and safer clinical option over the use of rhBMP2. © 2013 Orthopaedic Research Society Published by Wiley Periodicals, Inc. J Orthop Res XX:XXX–XXX, 2013

Keywords: BMP2; bone healing; critical size defect; microencapsulation; PEGDA

Successful repair of large bone defects in orthopedic trauma remains a clinical challenge. Although bone possesses repair capacity, it is often insufficient to overcome large bone loss. In most cases, surgical intervention is required to augment the bone healing process. Clinical approaches involve the use of vascularized and non-vascularized bone grafts or the application of growth factors such as recombinant human bone morphogenetic protein 2 (rhBMP2) and collagen to augment or provide a synthetic graft. However, both autologous and/or vascularized bone grafts are compromised by their limited availability and are typically associated with donor site morbidity.[1,2] The use of osteoinductive proteins such as rhBMP2, released in vivo to augment bone regeneration, has been developed for clinical use. Unfortunately, large amounts (6–12 mg) of rhBMP2 protein are required to achieve a reliable bone induction,[3–6] and delivery of the large amounts of this protein has led to production of antibodies as well as osteolysis of the bone often before it has completely repaired as well as other adverse effects.[7,8] To circumvent these problems much emphasis has been focused on linking the protein to a variety of matrixes that would allow for a slower release over time.[9] These systems are problematic due to the difficulty in crosslinking large amounts of the protein to the biomaterial, which would release the protein slowly over time in an active form.[10] For these reasons, molecular therapies to provide long-term secretion of BMP2 at physiological levels from human cells has been explored using a variety of systems including viral (retrovirus, adenovirus, and AAV) and non-viral (plasmids) gene delivery systems.[11–13] The limited transduction efficiency in vivo and risk of chromosomal integration have limited the potential of these approaches.

In this study, we developed a cell-based molecular therapy that allows the use of allogeneic cells transduced with AdBMP2, thus circumvent problems associated direct injection of viral vector and obviates the necessity of harvesting of autologous cells. Human cells were transduced ex vivo with a replication defective virus, thus the animals received no virus.[14,15] The cells are further wrapped in poly (ethylene glycol) diacrylate (PEGDA) hydrogel,[16] which has been previously shown to prevent immune detection.[17,18] PEGDA hydrogels are bio inert, hydrophilic polymeric networks widely used in tissue engineering applications.[19] This polymer is cross-linked through exposure to white light so that cells can be seeded without risk of thermal toxicity during crosslinking. The porous network of the PEGDA hydrogels allows for diffusion of gases and nutrients, allowing encapsulated cells to remain viable, while protecting the encapsulated cells from clearance by the immune system.[17,20] Previous research has also shown that injected PEGDA hydrogels also allow for sufficient release of therapeutic proteins, like insulin, for diabetic therapy and BMP2 for bone formation.[16,17,21,22] In our system, the polymer mesh size is such that BMP2 can diffuse out of the microbeads but neither immune-activated host

Grant sponsor: Defense Advanced Research Agency (DARPA); Grant number: W911NF-09-1-0040; Grant sponsor: Department of Defense Orthopedic Extremities Program (DAMD); Grant number: W81XWH-07-1-0215.
Correspondence to: Elizabeth A. Olmsted-Davis
(T: 713-798-1253; F: 713-798-1230; E-mail: edavis@bcm.edu)

cells nor immunoglobulin can diffuse in, therefore offering protection of the microencapsulated cells from the host immune system.

Here we extend these studies by demonstrating that delivery of low doses (96 ng/day) of endogenously produced BMP2 leads rapid and reliable bone formation and healing in a critical size femur defect. The rate of healing occurred as early as 3 weeks, or more rapid than similar experiments using high dose recombinant BMP2. In these studies injection of these microspheres into the void region led to rapid healing of a 5 mm femoral defect. This newly formed bone was well-integrated at the defect edges with the skeletal bone, and allowed the animals to ambulate normally without additional fixation as early as 2 weeks after delivery. These results indicate that these osteoinductive microspheres may be a safe and efficacious substitute for rhBMP2 and provide a clinically novel option to bone graft in the regeneration of traumatic bone defects.

MATERIALS AND METHODS

Cell Culture

Wistar skin fibroblasts (WSF) were generated from a skin biopsy from a Wistar rat. W20-17, a murine bone marrow stromal cell line, was obtained as a gift from Genetic Institute, Cambridge, MA and was propagated as previously described.[23] All cells were propagated in a humidified incubator at 37°C/5% CO_2 in Dulbecco's modified Eagle's medium (Sigma, St. Louis, MO) supplemented with 10% fetal bovine serum (HyClone, Logan, UT), 100,000 U/L penicillin, 100 mg/L streptomycin, 0.25 mg/L amphotericin B (Invitrogen Life Technologies, Gaithersburg, MD), and 3 mg/L tetracycline (Sigma).

Adenovirus and Cell Transduction

A replication defective first generation human type 5 adenovirus (Ad5) deleted in regions E1 and E3 was constructed to contain the cDNA for human BMP2 in the E1 region of the viral genome.[24] The control vector included the same adenovirus but lacked a transgene cassette (Ad5empty cassette). The virus particle (vp) to plaque-forming unit (pfu) ratios of Ad5BMP2 and Ad5empty cassette were 1:120 and 1:106, respectively, and all viruses were shown to be negative for replication-competent adenovirus. WSF were transduced with Ad5BMP2 or Ad5empty cassette control virus at a concentration of 7,500 vp/cell with GeneJammer.[25] Transduction efficiency was >90%.[25]

Microencapsulation

PEGDA was synthesized by reacting 10 kDa PEG with a twofold molar excess of acryloyl chloride as previously described.[16,20] Hydrogel precursor solutions were performed by combining 0.1 g/ml 10 kDa PEGDA (10% w/v) with 1.5% (v/v) triethanolamine/HEPES-buffered saline (pH 7.4), 37 mM 1-vinyl-2-pyrrolidinone, 0.1 nM eosin Y, 0.1% pluronic F68, and transduced WSF cells for a final concentration of 1×10^5 cells/μl. A hydrophobic photoinitiator solution (2,2-dimethoxy-2-phenyl acetophenone in 1-vinyl-2-pyrrolidinone; 300 mg/ml) was combined in mineral oil (3 μl/ml, embryo tested, sterile filtered; Sigma–Aldrich, St. Louis, MO). The microspheres were formed after adding the hydrogel precursor solution into the mineral oil, emulsifying by vortex for 2 s while exposing to white light for an additional 20 s. Microspheres were isolated through centrifugation at 330*g*.

Preparation of Cells for Injection in the Defect

Ad5BMP2 or Ad5empty cassette transduced cells were suspended in PBS and directly injected using a 22 gauge needle and syringe at a concentration of 5×10^7 cells per 1 ml of PBS. Microencapsulated cells were prepared at a concentration of 2×10^7 cells per 100 μl of hydrogel and a total volume of 1 ml of PBS containing microencapsulated cells were loaded into a syringe with an 18-gauge needle.

Quantification of BMP2 Protein and Activity After Transduction of Cells With Ad5BMP2

BMP2 protein was measured in culture supernatant 24 h after transduction of cells with Ad5BMP2 using a Quantikine BMP2 immunoassay ELISA kit (DBP200; R&D Systems, Minneapolis, MN). BMP2 biological activity was quantified in culture supernatant 24 after transduction by alkaline phosphatase (AP) assay using W20-17 cells.[26] Briefly, W20-17 cells were plated in 24-well plates at subconfluent density and 24 h later, the media was replaced with 200 μl of fresh media and 200 μl of conditioned culture media. W20-17 cells were then assayed 72 h later for AP activity using a chemiluminescence procedure as previously described.[24]

Rat Femur Critical Size Defect Model

Wistar rats between 9- and 11-week-old (350–440 g) were shaved, disinfected, and a linear incision made over the lateral aspect of the gluteal region of the rat from the palpable greater trochanter of the femur to just above the knee joint. The musculature was separated to expose the femur. Four 6´´ long 0.45´´ (1.1 mm) diameter end-threaded K wires were placed in the bone at a 90° angle: two in the proximal and two in the distal end of the femur 2 mm apart. All pins were securely anchored within a tubular external fixation device placed along the length of the femur. A 5 mm osteo-periosteal defect was made in the middle part of the bone using a high-speed burr. At the time of surgery, microencapsulated cells were then injected into the defect void by placement into a sutured muscle pocket. Animals were allowed to recover, and resume normal activity. Rats tolerated this device well with <5% loss of animals due to failure in the fixation. All treated rats were capable of walking and full weight bearing after surgery. Radiological, histological, and biomechanical analyses have been performed at various time points after surgery (2, 3, 6, 9, and 12 weeks). All animal studies were performed in accordance with the standards of Baylor College of Medicine, Department of Comparative Medicine, after review and approval of the protocol by the Institutional Animal Care and Use Committee (IACUC).

Radiographic Evaluation and Microcomputed Tomography

At various time point of the study, animals were radiographed while under anesthesia using an XPERT model faxitron (Kubtec, Fairfield, CT) in biplanar projections. Hind limb of the animal was set at an exposure of 15 s and acceleration voltage of 30 kV. Radiographic analyses were performed using microcomputed tomography (microCT) system. Specimens were scanned at 0.1 mm in plane resolution with 0.25 mm thick contiguous slices using a Stratec XCT

RESEARCH SA PLUS pQCT SCANNER from Orthometrix, Inc. (White Plains, NY). This scanner provides data calibrated to bone equivalent density. Three dimensional reconstructions and multi planar orthogonal reconstructions were used to visualize new bone bridging the defect.[27] Total volume of new bone within the defect as a function of time was calculated from 3D rendering using a mineral density threshold of 600 Hounsfield units.[28]

Biomechanical Analysis

Hind limbs (defect and intact contralateral) were harvested at 3 and 12 weeks ($n = 5$), soft tissues removed and the proximal and distal ends of the femurs embedded in poly (methyl methacrylate) (PMMA) perpendicular to their long axis and adjusted to a plumb line oriented to the center of rotation of the testing system (Universal MTS Bionix 3700). The specimens were mounted using clamps and torsion was applied in a displacement control mode at a constant rate of 0.5°/s in direction replicating femur external rotation. Torsional load-to-failure was calculated and stiffness established from the most linear region of the load–deflection curve and ultimate strength was defined as the peak load causing angular displacement >30°.

Histological Analysis

Animals were euthanized at 2, 3, 6, 9, or 12 weeks post-surgery, hind limbs isolated and external fixator removed leaving the pins in place. The whole limb was then formalin fixed and decalcified (Richard-Allan Scientific Decalcifying Solution, Thermo Scientific, Kalamazoo, MI) for 6 days. The remaining pins were removed, tissue was trimmed for mounting in the cassettes and then processed and paraffin embedded. Serial sections (4 μm) covering the whole femur area were prepared and every fifth section were stained with hematoxylin and eosin for histological analysis. The image reconstruction was done by assembling sequential images covering the whole area of interest (2× magnification each image).

Statistical Analysis

The results are reported as mean ± SD. For BMP2 ELISA and AP assay, $n = 6$ and a standard t-test determined significance $^{*}p < 0.005$, $^{***}p < 0.001$. For stiffness and strength data, $n = 3$ and a standard t-test were performed. For bone volume data, $n = 3$ and ANOVA test determined significance $^{*}p < 0.05$.

RESULTS

Bone Formation Within the Femur Defect Requires PEGDA Hydrogel

Figure 1A shows a schematic of our approach. Briefly, allogeneic skin fibroblasts were transduced with Ad5BMP2 and 24 h later microencapsulated through addition of a hydrogel precursor solution (PEGDA) in a mineral oil emulsion, forming cross-linked microsphere structures upon exposure to white light. This injectable therapy is delivered into the target site of a critical size defect in the rat femur. The femur was chosen because it is the largest weight-bearing bone in the body and is one of the most challenging for clinical repair. In this model, threaded pins were placed across the ends of the femur allowing for a 5 mm gap to be created in the midshaft of the bone. The pins were held in place by an external fixation device so that the rat could ambulate without either compression of the defect or significant motion. Osteoinductive microspheres are then directly injected into the femur defect (Fig. 1A). Each microsphere measures between 50 and 350 μs as shown in Figure 1B.

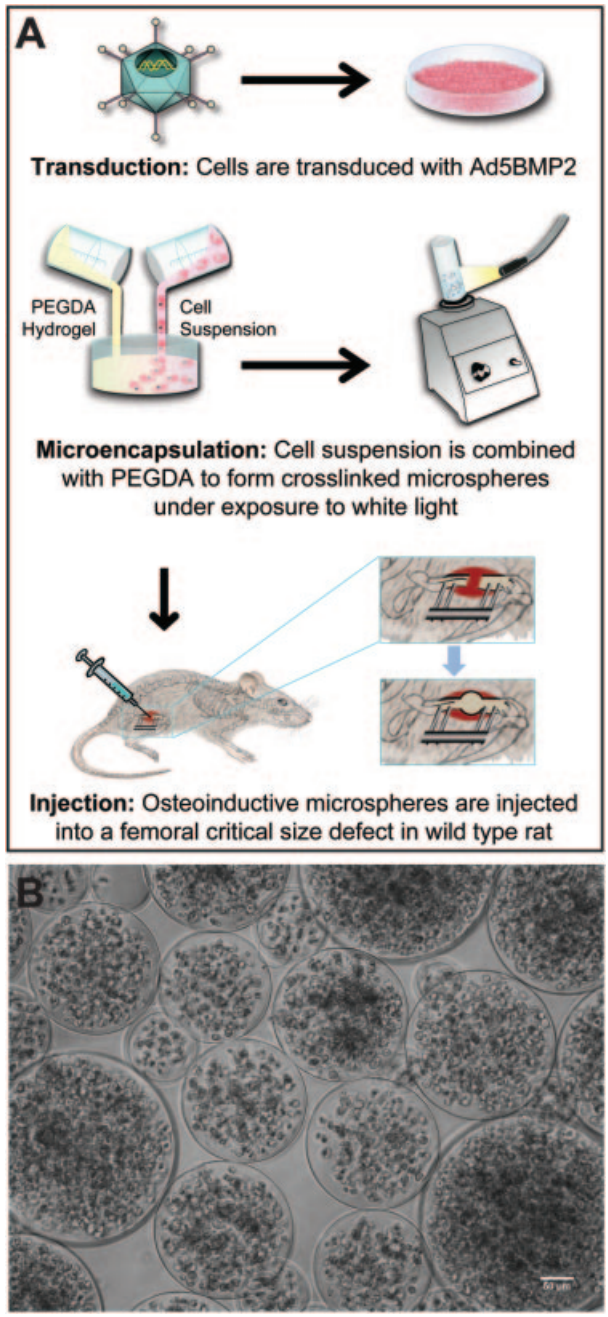

Figure 1. Manufacturing process of the injectable gene therapy. (A) Schematic depiction of the steps leading to the final osteoinductive microspheres. Briefly, allogeneic skin fibroblasts were transduced with Ad5BMP2 (7,500 vp/cell). Twenty-four hours later, the cells are collected and then combined with the PEGDA hydrogel precursor solution and microencapsulated through an emulsion technique using mineral oil. Crosslinking is achieved via a dual photoinitiator and exposing to white light as described in Olabisi.[16] The osteoinductive microspheres are then easily injected into the target site. (B) Phase contrast imaging of the cells microencapsulated in PEGDA hydrogel microspheres; 10× magnification.

We first performed dose escalation studies. No bone formation was observed in the defect in animals receiving 2×10^6 encapsulated cells (Fig. 2A) whereas complete healing was achieved with 2×10^7 microencapsulated cells (Fig. 2B). Quantitation of BMP2 levels released from osteoinductive microspheres in culture indicate that 48 ng of BMP2 was produced per 10^7 encapsulated cells over a 24 h period (Fig. 2E). Upregulation of endogenous cellular AP activity is commonly used for the assessment of osteogenic differentiation of stem cells.[26,29] AP assay showed that BMP2 produced by the microspheres possesses bioactivity similar to the recombinant protein (Fig. 2F). We next evaluated bone formation and healing in the defect using the osteoinductive microspheres, as compared to a similar number of Ad5BMP2 transduced cells, which were not encapsulated in PEGDA hydrogel. When encapsulated BMP2-producing cells were directly injected into the defect, there was no apparent bone formation and/or healing (Fig. 2C); while the same cells, when microencapsulated, were able to induce bone formation (Fig. 2D). As expected, there was no bone healing in control animals that received Adempty transduced cells microencapsulated in the PEGDA hydrogel and the defect formed a non-union fracture (data not shown).

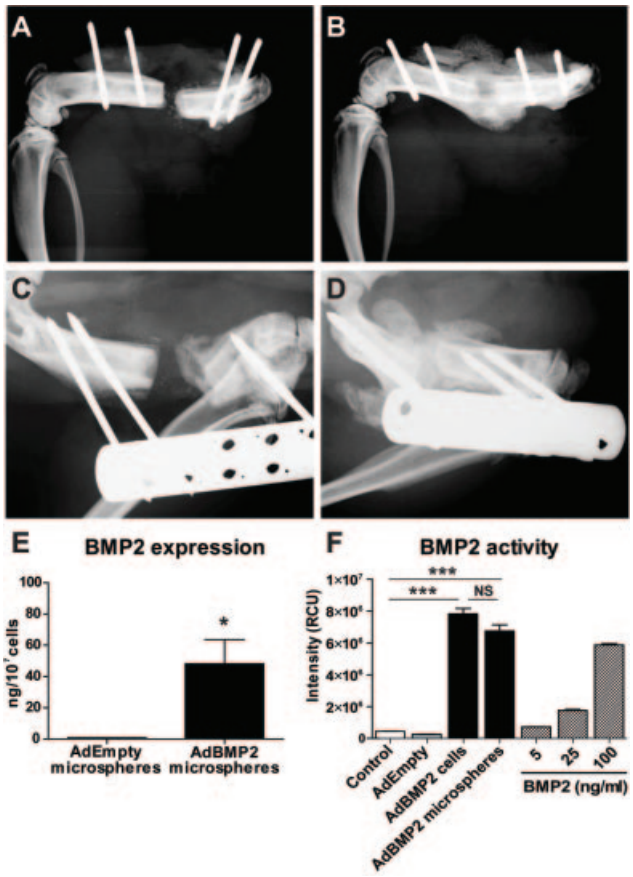

Figure 2. Osteoinductive microspheres induce bone formation in a model of femoral critical size defect in rat. (A and B) Radiographs 3 weeks after introduction of critical size defect in the rat femur and delivery of varying numbers of BMP2 expressing cells within microspheres; (A) 2×10^6 cells and (B) 2×10^7 cells. (C and D) Radiographs at 2 weeks after surgery and after injection of Ad5BMP2 transduced cells (C) or microencapsulated Ad5BMP2 transduced cells (D). (E) ELISA showing the amount of BMP2 protein required for response. Statistically significant changes, as denoted by an asterisk, were determined using a standard t-test; $^{*}p = 0.0401$; $n = 6$. (F) Alkaline phosphatase activity in W20-17 cells after addition of conditioned media from Ad5BMP2- or Ad5Empty cassette-transduced cells (7,500 vp/cell) in monolayer or microencapsulated (microspheres). Statistically significant changes, as denoted by an asterisk, were determined using a standard t-test; $^{***}p < 0.0001$; NS, $p = 0.0781$; $n = 6$.

New Bone Bridged the Defect and Integrated With Native Bone

Consistent bone formation was observed at the targeted site at 3 weeks after surgery by X-ray (Fig. 3A) and microCT (Fig. 3F). At this time there was bone bridging the defect in 95% of the animals compared to 76% at 2 weeks (Fig. 3K). This bridging bone did not appear to have a cortical exterior (Fig. 3F) but rather a more immature trabecular nature. However, by 6 weeks (Fig. 3B and G) the new bone appeared to have a cortical exterior and trabecular interior that bridged the defect without gaps. This bone remained consistent in samples isolated at later time points 6–12 weeks (Fig. 3B–D and G– I). The bone formation appeared finite rather than continually invasive and all rats continued to appear healthy, ambulate normally, and had no additional injuries. Neither bone formation nor spontaneous healing was observed in any of the seven control animals (Fig. 3E and J).

Bone healing was studied longitudinally, in a subset of animals, to evaluate any changes or adverse events occurring from injection of microspheres (Fig. 4). In these studies the external fixator was removed 2 weeks after surgery without disruption of the newly forming bone (Fig. 4A), and the rat was X-rayed, and then followed radiographically at 2, 4, 12, 22, 34, and 45 weeks (Fig. 4A–F). The shape of the new bone did not change significantly from 2 weeks to 11 months, as seen in Figure 4. However, the bone became more mineralized with time, suggesting that remodeling was occurring.

When analyzed by histology bone filled the defect at 3 weeks (Fig. 5A). Microspheres were observed at the periphery and newly formed bone is also observed around the microspheres within the defect. No accute inflammatory reaction was observed within the newly forming callus or tissues surrounding the microspheres. Interestingly, new bone appears to be integrated or fused with the intact femur suggesting complete bone healing and supporting the results seen by microCT. However, at 3 weeks, some areas of cartilage and immature bone were observed. Also at 3 weeks bone appeared to be less remodeled, although there was the appearance of early cortical bone at the defect edges, suggesting the callus is still undergoing remodeling. At 6 weeks, the bone appeared to be more remodeled, with a cortical exterior and internal marrow cavity. Although immature bone -mineralized

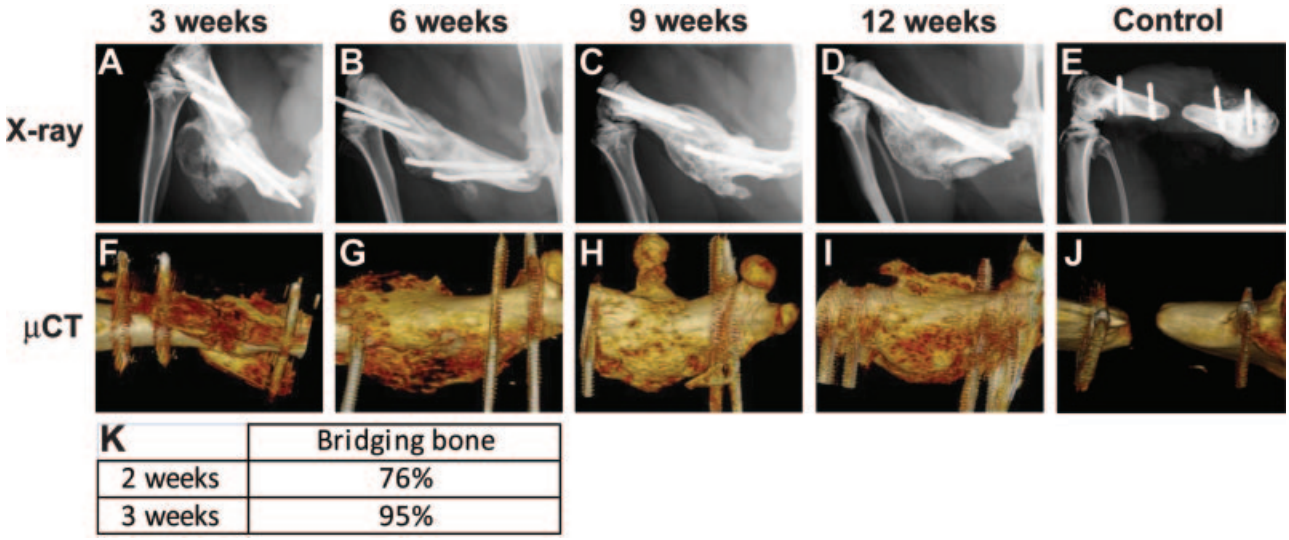

K	Bridging bone
2 weeks	76%
3 weeks	95%

Figure 3. Radiological analysis at 3, 6, 9, and 12 weeks after surgery. (A–E) X-ray images and (F–J) 3D surface renderings obtained from micro-computational analysis of the bone formation within the defect at 3 weeks (A and F), 6 weeks (B and G), 9 weeks (C and H), and 12 weeks (D and I) after surgery. Controls as a 12 weeks after surgery are shown in (E) and (J). (K) Radiographic assessment of samples which had bone bridging the defect at 2 and 3 weeks after surgery (expressed in percentage, $n = 21$).

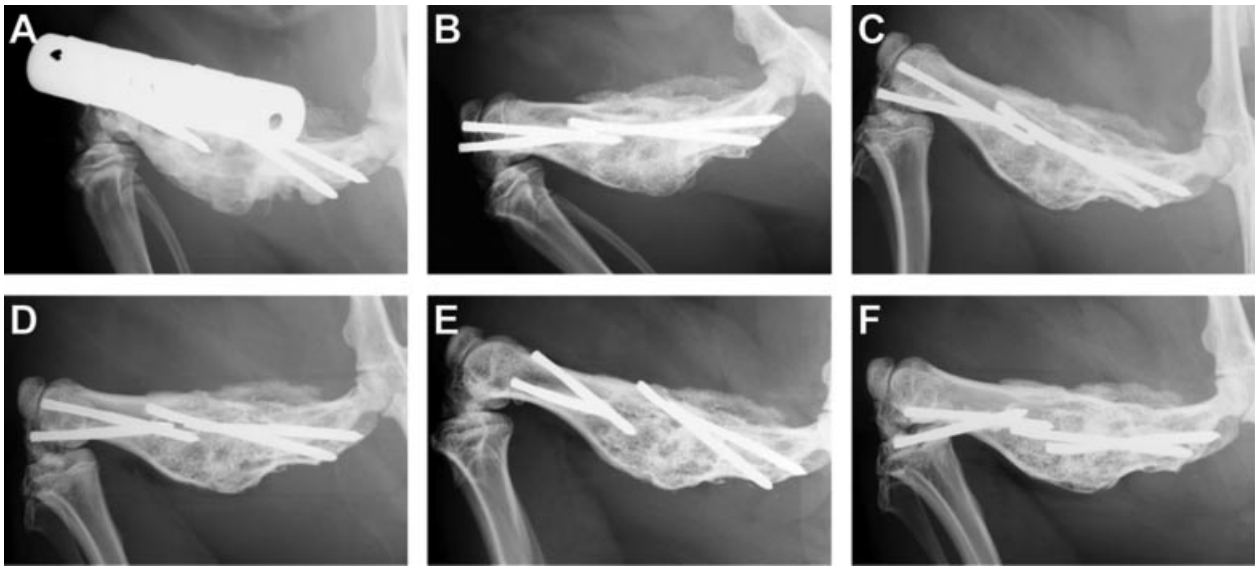

Figure 4. Longitudinal radiographic analysis of bone repair in the femoral defect model. Microspheres possessing Ad5BMP2 transduced cells were injected immediately following introduction of the 5 mm femur defect, and resultant bone healing followed over the course of 45 weeks. Bone formation appears to remodel and become more mineralized initially; (A) 2 weeks, (B) 4 weeks, and (C) 12 weeks, after which the bone was stable and did not appear to undergo additional remodeling or resorption (D) 22 weeks, (E) 34 weeks, (F) 45 weeks after surgery.

cartilage was still observed (Fig. 5B). At 12 weeks, no more cartilage is seen in the area of newly formed bone (Fig. 5C), and there is now a well-developed cortical exterior and trabecular interior as noted in the microCT images. Although not shown in this photomicrograph there was a contiguous marrow cavity.

Biomechanical Analysis of the New Bone, Suggests That It Rapidly Obtains Strength Comparable to the Intact Femur

Biomechanical torsional testing was performed on the contralateral intact and defect femurs isolated from the rats 3 and 12 weeks after surgery. The average torsional stiffness at 3 and 12 weeks were 0.026 ± 0.011 and 0.061 ± 0.015 N m/degree and 93% and 121% of the contralateral intact femur, respectively (Fig. 6A). The average torsional strength at 3 weeks was 0.35 ± 0.13 N m yielding 79% of the contralateral intact femur (Fig. 6B). The defect femur strength persisted and at 12 weeks, the average torsional strength was 0.41 ± 0.12 N m or 75% of the contralateral femur, suggesting that bone was continuing to be maintained within the defect. There was no statisti-

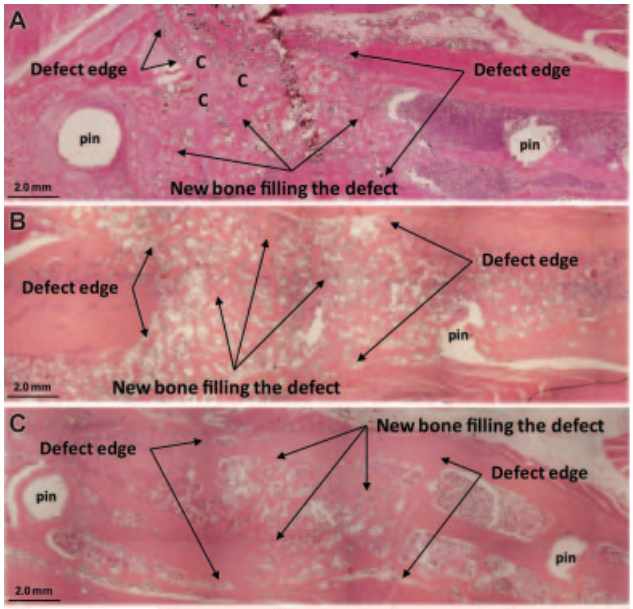

D	3 weeks	6 weeks	9 weeks	12 weeks
Cartilage	+++	+	+/-	-
New bone	++	+++	+++	+++
Marrow cavity	-	+/-	+	++

Figure 5. Histological analysis at bone repair of the femoral defect. The hind limb of interest has been harvested, formalin fixed paraffin embedded, serial sectioned, and every 5th section stained with hematoxylin and eosin. Representative photomicrograph of bone healing in the femoral defect at 3 weeks (A), 6 weeks (B), and 12 weeks (C) post-injection of osteoinductive microspheres. The photomicrograph is a montage of representative images taken at 2× magnification through the entire defect region. The defect edges are highlighted with arrows. We observed substantial amount of immature bone filling the defect. Calcified cartilage was also observed within the central callus. Holes within the femur ends represent the location of the bone pins used for the external fixation, which were removed prior to tissue processing. (D) Histologic assessment of samples which had cartilage, new bone formation, and/or presence of marrow cavity at various times after injection of osteoinductive microspheres.

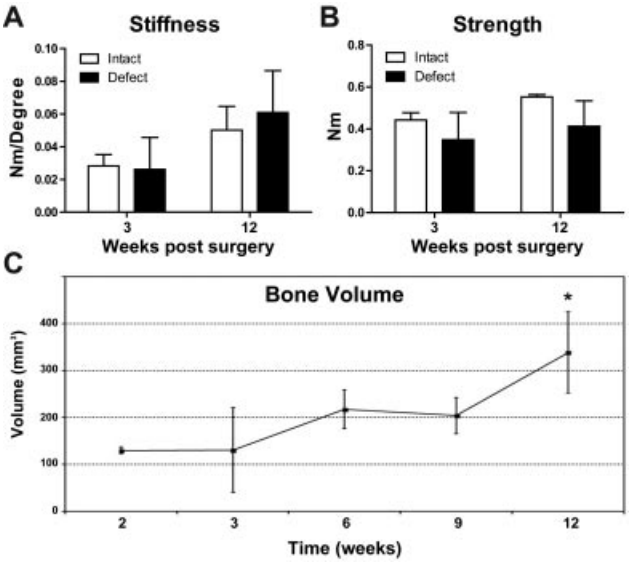

Figure 6. Biomechanical analysis of bone healing in the femoral defect model. (A and B) Graphical depiction of torsional stiffness (A) and strength (B) of femur defect and intact contralateral femur at 3 and 12 weeks after surgery. Statistical analysis (t-test) demonstrated no statistically significant difference in stiffness and strength between defect and intact femur specimens at 3 ($p = 0.8021$ and $p = 0.4974$, respectively; $n = 3$) or 12 weeks ($p = 0.2781$ and $p = 0.3390$, respectively; $n = 3$). (C) Graph representing the mean volume of the new bone formed within and around the defect at 2, 3, 6, 9, and 12 weeks after surgery. The density threshold of 600 shows highly mineralized bone. Statistically significant changes, as denoted by an asterisk, were determined using ANOVA test; $^{*}p = 0.0181$; $n = 3$.

cally significant difference in stiffness and strength between defect and intact femur at 3 versus 12 weeks ($p = 0.2781$ and $p = 0.3390$, respectively).

MicroCT demonstrated well-mineralized bone formed within the defect as early as 3 weeks post-surgery. The new bone bridged the defect and was seamlessly integrated with the native bone at the defect ends. The process of new bone formation was robust, consistent, and conformed to defect site. The new bone exhibited homogeneity in morphology and the mineral content. At 2, 3, 6, 9, and 12 weeks intervals post-surgery, a steady increase in the average volume of new bone formation within the defect was observed (Fig. 6C). There was statistically significant twofold increase in average volume of new bone in the defect throughout the course of the experiment (2 weeks vs. 12 weeks, $p = 0.0181$). Furthermore, this increase in new volume correlated well with the tortional strength of the defect treated with osteoinductive microspheres ($R^2 = 0.6084$, $p = 0.025$).

DISCUSSION

The data collectively demonstrates rapid bone healing of a critical size femur defect in wild type rats after injection of osteoinductive microspheres. Our approach shows considerable benefits compared to other studies using BMP2.

First, we employ cells that continually express lower levels of BMP2 (96 ng/day) which are approximately 100-fold lower than similar studies using recombinant protein. This level of BMP2 is similar to the amount of protein that is incorporated and potentially released from bone during fracture.[30] We have previously shown that transgene expression from the cells was sustained and locally retained within the microspheres for up to 15 days.[16] Thus, the sustained delivery of BMP2 at these lower levels will potentially avoid adverse events associated with the recombinant BMP2 protein.

Secondly, these osteoinductive microspheres rely on transduction of allogeneic cells as "carriers" for the BMP2 transgene. Since these cells cannot contribute directly to the bone formation, due to the PEGDA hydrogel encapsulation, there is no requirement for including stem cell populations and thus allows for the use of a previously qualified allogeneic cell line. Therefore, there is no limitation in the cell source and the materials can be manufactured and cryopreserved[31] so that they are ready at the desired time of surgery.

These studies are the first proof of concept studies that low sustained delivery of BMP2 can lead to reliable and rapid bone heals a critical size femur defect in rats. Delivery of the microspheres resulted in rapid new bone formation only in the targeted bone void region. The results of biomechanical testing suggested that the callus was well-integrated with the pre-existing skeletal bone with torsional strength and stiffness recovering to 79% and 93%, respectively, as compared with the intact contralateral femur. This reacquisition of strength and stiffness is dramatic and appears as early as 3 weeks after the injection of the osteoinductive microspheres. The new bone formation within the defect was also followed through microCT and found to be increasing even at latter time points where histology did not show significant cartilage. This may in part be due to continued conversion of cartilage and immature bone to more well-mineralized bone. However, significant variation within each animal group suggests that the rate of bone formation and remodeling may be somewhat animal dependent. Previous studies using high dose recombinant BMP2 did not obtain similar bone repair before 12 weeks.[32] The data again, suggests that the sustained expression of BMP2 at physiological levels may be significantly more effective at bone healing than its recombinant counterpart.

Histological evaluation of the callus appeared to progress as expected in fracture repair, with only minor amounts of cartilage detectable after 6 weeks. The bone appeared to undergo some remodeling exhibiting a uniform trabecular nature at 2 weeks to a more organized structure with a cortical exterior and remodeled bone marrow cavity that becomes apparent in the 6-week samples. The integration of new bone with the previous skeletal bone was observed as early as 2 weeks and longitudinal X-rays of femur healing showed that after 6 weeks the bone appeared to have a stable shape and size. Interestingly, the bone did not return to the exact shape of the contralateral femur, which may be in part due to the presence of the nonresorbable microbeads that remain in the location for up to 2–3 years within the newly formed bone. However the bone was stable and we observed no other adverse events associated with the animals even as long as 11 months.

This system holds potential for clinical translation. We recently have found that this system is capable of inducing soft tissues regeneration, including the rapid generation of new vasculature and nerves.[15,33,34] These studies confirmed that our system was capable of recapitulating the biological functions of endogenous BMP2. Thus, these microspheres may also provide substantial soft tissue benefits. Further, antibiotics such as vancomycin could easily be incorporated into the PEG to provide a mechanism for treatment of infection. Thus, delivery of these microspheres may provide benefit towards both bone and soft tissue regeneration which is essential for functional limb salvage.

Current clinical approaches for healing traumatic bone injuries involve a multi-step process by which the bone defect is maintained with a spacer, while the soft tissues are allowed stabilize and infection is treated.[35] With the unique properties of the PEGDA hydrogel, the microspheres could be injected multiple times without launching a secondary immune response. Therefore, the microspheres could be delivered several times to augment current clinical approaches or alternatively, could be engineered to potentially provide a one-step process. In addition to the potential to incorporate antibiotics, these microspheres can be designed to be totally degradable, through inclusion of a cellular "safety switch" that will induce cellular apoptosis in the carrier cells before the hydrogel degradation. The biomaterial can then be selectively degraded through inclusion of specific protease sites, that allow for tunable degradation after the injury is healed.[36] Finally, we have already demonstrated the ability for these microspheres to be cryopreserved, without change in efficacy, and thus could be easily manufactured and distributed clinically.[31]

ACKNOWLEDGMENTS

This work was supported in part by grants from Defense Advanced Research Agency (DARPA) W911NF-09-1-0040 and Department of Defense Orthopedic Extremities Program (DAMD) W81XWH-07-1-0215. The authors thank Angie Fuentes for performing the microcomputer tomography, Rita Nistal for the histology, and Francis Gannon for his advices on histology.

REFERENCES

1. Summers BN, Eisenstein SM. 1989. Donor site pain from the ilium. A complication of lumbar spine fusion. J Bone Joint Surg Br 71:677–680.
2. Seiler JG III, Johnson J. 2000. Iliac crest autogenous bone grafting: donor site complications. J South Orthop Assoc 9:91–97.
3. Govender S, Csimma C, Genant HK, et al. 2002. Recombinant human bone morphogenetic protein-2 for treatment of open tibial fractures: a prospective, controlled, randomized study of four hundred and fifty patients. J Bone Joint Surg Am 84-A:2123–2134.
4. Hwang CJ, Vaccaro AR, Lawrence JP, et al. 2009. Immunogenicity of bone morphogenetic proteins. J Neurosurg Spine 10:443–451.
5. Winn SR, Hu Y, Sfeir C, et al. 2000. Gene therapy approaches for modulating bone regeneration. Adv Drug Deliv Rev 42:121–138.
6. Jeon O, Song SJ, Kang SW, et al. 2007. Enhancement of ectopic bone formation by bone morphogenetic protein-2 released from a heparin-conjugated poly(L-lactic-co-glycolic acid) scaffold. Biomaterials 28:2763–2771.
7. Carragee EJ, Hurwitz EL, Weiner BK. 2011. A critical review of recombinant human bone morphogenetic protein-2 trials in spinal surgery: emerging safety concerns and lessons learned. Spine J 11:471–491.
8. Kang JD. 2011. Another complication associated with rhBMP-2? Spine J 11:517–519.

9. Hutmacher DW, Woodruff MA, Shakesheff K, et al. 2012. Direct fabrication as a patient-targeted therapeutic in a clinical environment. Methods Mol Biol 868:327–340.
10. Lutolf MP, Weber FE, Schmoekel HG, et al. 2003. Repair of bone defects using synthetic mimetics of collagenous extracellular matrices. Nat Biotechnol 21:513–518.
11. Moutsatsos IK, Turgeman G, Zhou S, et al. 2001. Exogenously regulated stem cell-mediated gene therapy for bone regeneration. Mol Ther 3:449–461.
12. Chen Y, Luk KD, Cheung KM, et al. 2003. Gene therapy for new bone formation using adeno-associated viral bone morphogenetic protein-2 vectors. Gene Ther 10:1345–1353.
13. Musgrave DS, Bosch P, Ghivizzani S, et al. 1999. Adenovirus-mediated direct gene therapy with bone morphogenetic protein-2 produces bone. Bone 24:541–547.
14. Olmsted-Davis E, Gannon FH, Ozen M, et al. 2007. Hypoxic adipocytes pattern early heterotopic bone formation. Am J Pathol 170:620–632.
15. Dilling CF, Wada AM, Lazard ZW, et al. 2010. Vessel formation is induced prior to the appearance of cartilage in BMP-2-mediated heterotopic ossification. J Bone Miner Res 25:1147–1156.
16. Olabisi RM, Lazard ZW, Franco CL, et al. 2010. Hydrogel microsphere encapsulation of a cell-based gene therapy system increases cell survival of injected cells, transgene expression, and bone volume in a model of heterotopic ossification. Tissue Eng A 16:3727–3736.
17. Pathak CP, Sawhney AS, Hubbell JA. 1992. Rapid photopolymerization of immunoprotective gels in contact with cells and tissue. J Am Chem Soc 114:8311–8312.
18. Cruise GM, Hegre OD, Lamberti FV, et al. 1999. In vitro and in vivo performance of porcine islets encapsulated in interfacially photopolymerized poly(ethylene glycol) diacrylate membranes. Cell Transplant 8:293–306.
19. Ratner BD, Hoffman AS, Schoen FJ, et al. 2004. An introduction to materials in medicine. Biomater Sci Chapter II:100–107.
20. Franco CL, Price J, West JL. 2011. Development and optimization of a dual-photoinitiator, emulsion-based technique for rapid generation of cell-laden hydrogel microspheres. Acta Biomater 7:3267–3276.
21. Cruise GM, Scharp DS, Hubbell JA. 1998. Characterization of permeability and network structure of interfacially photopolymerized poly(ethylene glycol) diacrylate hydrogels. Biomaterials 19:1287–1294.
22. Bikram M, Fouletier-Dilling C, Hipp JA, et al. 2007. Endochondral bone formation from hydrogel carriers loaded with BMP2-transduced cells. Ann Biomed Eng 35:796–807.
23. Thies RS, Bauduy M, Ashton BA, et al. 1992. Recombinant human bone morphogenetic protein-2 induces osteoblastic differentiation in W-20-17 stromal cells. Endocrinology 130:1318–1324.
24. Olmsted EA, Blum JS, Rill D, et al. 2001. Adenovirus-mediated BMP2 expression in human bone marrow stromal cells. J Cell Biochem 82:11–21.
25. Fouletier-Dilling CM, Bosch P, Davis AR, et al. 2005. Novel compound enables high-level adenovirus transduction in the absence of an adenovirus-specific receptor. Hum Gene Ther 16:1287–1297.
26. Blum JS, Li RH, Mikos AG, et al. 2001. An optimized method for the chemiluminescent detection of alkaline phosphatase levels during osteodifferentiation by bone morphogenetic protein 2. J Cell Biochem 80:532–537.
27. Rosset A, Spadola L, Ratib O, et al. 2004. An open-source software for navigating in multidimensional DICOM images. J Digit Imaging 17:205–216.
28. Hoff BA, Kozloff KM, Boes JL, et al. 2012. Parametric response mapping of CT images provides early detection of local bone loss in a rat model of osteoporosis. Bone 51:78–84.
29. Jaiswal N, Haynesworth SE, Caplan AI, et al. 1997. Osteogenic differentiation of purified, culture-expanded human mesenchymal stem cells in vitro. J Cell Biochem 64:295–312.
30. Urist MR, Mikulski A, Lietze A. 1979. Solubilized and insolubilized bone morphogenetic protein. Proc Natl Acad Sci USA 76:1828–1832.
31. Mumaw J, Jordan ET, Sonnet C, et al. 2012. Rapid heterotrophic ossification with cryopreserved poly(ethylene glycol-) microencapsulated BMP2-expressing MSCs. Int J Biomater 2012:861794.
32. Kolambkar YM, Dupont KM, Boerckel JD, et al. 2011. An alginate-based hybrid system for growth factor delivery in the functional repair of large bone defects. Biomaterials 32:65–74.
33. Salisbury E, Rodenberg E, Sonnet C, et al. 2011. Sensory nerve induced inflammation contributes to heterotopic ossification. J Cell Biochem 112:2748–2758.
34. Salisbury E, Lazard Z, Ubogu EE, et al. 2012. Transient brown adipocyte-like cells derive from peripheral nerve progenitors in response to bone morphogenetic protein 2. Stem Cells Transl Med 12:874–885.
35. Donegan DJ, Scolaro J, Matuszewski PE, et al. 2011. Staged bone grafting following placement of an antibiotic spacer block for the management of segmental long bone defects. Orthopedics 34:e730–e735.
36. Hsu CW, Olabisi RM, Olmsted-Davis EA, et al. 2011. Cathepsin K-sensitive poly(ethylene glycol) hydrogels for degradation in response to bone resorption. J Biomed Mater Res A 98:53–62.